Multi-Band Full Duplex MAC Protocol (MB-FDMAC)

Yazeed Alkhrijah[®], Member, IEEE, Joseph Camp[®], Member, IEEE, and Dinesh Rajan, Senior Member, IEEE

Abstract—In this paper, we propose a multi-band medium access control (MAC) protocol for an infrastructure-based network with an access point (AP) that supports In-Band full-duplex (IBFD) and multiuser transmission to multi-band-enabled stations. The Multi-Band Full Duplex MAC (MB-FDMAC) protocol mainly uses the sub-6 GHz band for control-frame exchange, transmitted at the lowest rate per IEEE 802.11 standards, and uses the 60 GHz band, which has significantly higher instantaneous bandwidth, exclusively for data-frame exchange. We also propose a selection method that ensures fairness among uplink and downlink stations. Our result shows that MB-FDMAC effectively improves the spectral efficiency in the mmWave band by 324%, 234%, and 189% compared with state-of-the-art MAC protocols. In addition, MB-FDMAC significantly outperforms the combined throughput of sub-6 GHz and 60 GHz IBFD multiuser MIMO networks that operate independently by more than 85%. In addition, we study multiple network variables such as the number of stations in the network, the percentage of mmWave band stations, the size of the contention stage, and the selection method on MB-FDMAC by evaluating the change in the throughput, packet delay, and fairness among stations. Finally, we propose a method to improve the utilization of the high bandwidth of the mmWave band by incorporating time duplexing into MB-FDMAC, which we show can enhance the fairness by 12.5 % and significantly reduces packet delay by 80%.

Index Terms—Full duplex, MU-MIMO, MAC, WLAN, multiband, IEEE 802.11be, IEEE 802.11ay.

I. INTRODUCTION

PID growth of data-intensive applications, such as virtual reality, high-definition streaming, and video gaming, has resulted in an unprecedented surge in traffic demand. For example, Cisco has projected the percentage of ultra-high-definition TVs that will connect to the internet in 2023 to reach 66% of connected TVs, up from 33% in 2018 [1], and their internet usage has soared from 12704 petabytes per month in 2016 to 42255 petabytes per month in 2021 [2]. In addition, the majority of these devices use a Wireless Local Area Network (WLAN). By 2023, Cisco estimates that 75% of the devices in North America will use WLANs to access the internet [1]. Consequently, researchers have been actively investigating

Manuscript received 20 October 2022; revised 28 February 2023; accepted 11 April 2023. Date of publication 21 June 2023; date of current version 21 August 2023. The work has been supported by Imam Mohammad Ibn Saud Islamic University (IMISU) (IMISU-RP23123). (Corresponding author: Yazeed Alkhrijah.)

Yazeed Alkhrijah is with the Department of Electrical Engineering, Imam Mohammed Ibn Saud Islamic University (IMISU), Riyadh 11432, Saudi Arabia (e-mail: yalkhrijah@smu.edu).

Joseph Camp and Dinesh Rajan are with the Department of Electrical and Computer Engineering, Southern Methodist University, Dallas, TX 75205 USA.

Color versions of one or more figures in this article are available at https://doi.org/10.1109/JSAC.2023.3287546.

Digital Object Identifier 10.1109/JSAC.2023.3287546

innovative techniques that can significantly augment transmission rates and enhance spectral efficiency. In this work, we propose a new medium access control (MAC) protocol that integrates three key ideas, namely multi-band operation, in-band full duplex (IBFD), and multiuser beamforming, to meet the increasing traffic demand.

WLAN typically operates in two frequency bands. The first is the sub-6 GHz microwave (μ Wave) band. The second is the millimeter wave (mmWave) band, which operates around 60 GHz frequencies. The μ Wave band has a higher coverage area than the mmWave band, whereas the available instantaneous bandwidth for the latter results in much higher data throughput. With the advances in antenna design and integrated circuit technology, user equipment (UE) can operate simultaneously in multiple frequency bands and has small form factors [3]. Researchers in [4], [5], [6], [7], [8], [9], [10], [11], [12], [13], and [14] have considered the joint use of μ Wave and mmWave bands to leverage the higher instantaneous bandwidth of the mmWave band and the larger covered area by the μ Wave band.

MuMIMO is another key enabler for gigabit transmission in WLANs. With a given number of antennas, the access point (AP) can simultaneously broadcast data to multiple stations. Also, the AP can decode signals from multiple uplink stations with the same configuration. As a result, MuMIMO increases the overall throughput since multiple simultaneous transmissions occur. Also, MuMIMO improves the diversity gain compared to single-user MIMO by increasing the immunity to channel rank loss and antenna correlation [15]. Also, MuMIMO can be achieved without multiple antennas at the stations (only at the AP), which reduces the implementation cost [16].

IBFD enables a node to transmit and receive data simultaneously using a single frequency and has the potential to double the overall spectral efficiency [17]. In addition, IBFD improves security by obfuscating any eavesdropper with multiple transmitted signals on a single frequency [18]. Also, IBFD reduces the end-to-end transmission delay and solves the hidden terminal and exposed terminal problems [19]. Canceling self-interference (SI) is the main challenge in enabling IBFD. Recently, numerous works have been proposed to suppress SI by combining propagation, analog, and digital SI cancellation techniques, making IBFD feasible [20]. Several sophisticated MAC protocols have been proposed to mitigate the SI and maximize the throughput for IBFD [17], [18], [19], [20], [21], [22], [23], [24], [25], [26].

The main contributions of this paper are as follows.

 We design a new multi-band infrastructure-based MAC that utilizes IBFD and multiuser transmission to serve

0733-8716 © 2023 IEEE. Personal use is permitted, but republication/redistribution requires IEEE permission. See https://www.ieee.org/publications/rights/index.html for more information.

multiple uplink and downlink stations simultaneously in two bands. The first frequency band is a low-frequency (i.e., sub-6 GHz or μ Wave) band that is mainly used for control frame exchange, and the second is a high-frequency (i.e., mmWave) band that is used for data frame exchange. The MB-FDMAC design is based on the latest IEEE 802.11ax and 802.11ay standards for the sub-6 GHz band and mmWave band, respectively. MB-FDMAC also supports data transmission on the sub-6 GHz band, as a special case, for stations outside the mmWave range. Also, MB-FDMAC switches to the half-duplex mode when IBFD is not feasible, for instance, due to the high inter-user interference levels.

- We compare the performance of MB-FDMAC with sub-6 GHz and mmWave systems that each support MuMIMO and IBFD but operate independently to quantify the effectiveness of the proposed multi-band approach. The MB-FDMAC throughput is 87% higher than the combined throughput of sub-6 GHz and mmWave bands. Also, we show that MB-FDMAC increases the throughput by 101% compared with a modified version of the protocol that works in half-duplex mode.
- We propose a multi-band station selection scheme (MB-JSS) that considers fairness in the station selection decision. Also, we use two baseline selection schemes for comparison: random and opportunistic user selection. We show that MB-JSS achieves a saturation throughput close to the random selection scheme. Also, we show that MB-JSS reduces the average packet delay by more than 95% and improves fairness by more than 200% compared with the baselines.
- We include another feature in MB-FDMAC that better utilizes the large instantaneous bandwidth of the mmWave band by dividing the transmission period into multiple time segments to serve more stations in each transmission period in both the uplink and downlink directions. This feature also increases the efficiency of the mmWave band with stations that send relatively small packets. Also, we show that this feature significantly reduces the average packet delay and increases the uplink and downlink fairness by 12.5% and 5%, respectively, with a marginal reduction in the throughput.

The rest of the paper is organized as follows. We discuss the related work in Section II. In Section III, we present the system model and the MAC design requirements. Then, we introduce the MB-FDMAC frame structure and station selection procedures in Section IV and Section V, respectively. In Section VI, we present the results of extensive simulations of MB-FDMAC. Finally, we conclude the paper in Section VII.

Notations: We use boldface capital and small letters to express matrices and vectors, respectively. We use \mathbf{X}^{T} and \mathbf{X}^{H} to denote the transpose and the Hermitian form of a matrix \mathbf{X} . We use scripted capital and lower-case letters to denote sets and elements receptively. Finally, (|. |) is the determinant operation.

II. RELATED WORK

There are three areas that are related to this work.

A. Wireless Local Area Network (WLAN) MAC Protocols

To enable the wide operation of WLAN, IEEE 802.11 was published as the main standard for WLAN in 1997. Subsequently, the standard was revised multiple times, and currently, IEEE 802.11ax (commercially named WIFI6) is used for the μ Wave band, and IEEE 802.11ay (commercially named WiGig) is used for the mmWave band. These latest standards utilize several new techniques, such as multi-input multi-output (MIMO), orthogonal frequency multiple access (OFDMA), and MuMIMO, to increase the spectral diversity and improve the sum rate of the system. Also, several new techniques - such as IBFD, multi-AP coordination, and multi-band operation- are considered in the next IEEE802.11 standards [27] [28].

The fundamental MAC protocol for IEEE 802.11 is the distributed coordination function (DCF). The basic idea of the DCF is to use the four-way handshake technique that operates as follows. First, the station with data sends a request-to-send (RTS) frame to the AP. Then, the AP replies with a clear-to-send (CTS) frame to the station. After that, the station transmits data to the AP. Finally, the AP sends an acknowledgment (ACK) frame to the station, confirming the successfulness of the transmission. This function is used universally with some modifications to suit the new WLAN techniques. However, the IEEE802.11 strictly enforces using the lowest transmission rate to send the control frames (i.e., RTS, CTS, and ACK frame) even if the station supports a higher transmission rate, resulting in inefficient utilization of the bandwidth.

B. Multi-Band Operation

The advancement of antenna technologies enabled small form factor devices to support μ Wave and mmWave simultaneously. However, the current WLAN standards do not include multi-band cooperation; instead, they make the devices use each band separately. Fortunately, the new WLAN task group (IEEE 802.11be or WIFI-7) is considering including multi-band cooperation in the next generation of WLANs.

In the literature, there are several methods for a node to use multiple bands cooperatively. The authors in [4] suggested using dual-band operations as a high-frequency communication enabler such that the UE sends a signal by using the μ Wave, and then the base station (BS) evaluates the feasibility of using the high-frequency band. Also, the dual-band operation is leveraged to estimate the UE's mmWave channel using sub-6 GHz signals in [5]. In addition, the authors of [7] propose using the sub-6 GHz band as a control channel for the beam alignment phase in the mmWave band. The authors of [8] suggest using two bands for simultaneous data transmission. Also, the authors of [9] proposed a scheduler that uses multi-band operation on the transport layer to increase reliability and improve the system throughput. Also, the WLAN operation over sub-6 GHz and mmWave bands are leveraged in [10] to allocate data transmission in an idle band if the other band is busy. Similarly, the authors of [11] propose a dynamic traffic allocator. Furthermore, the authors of [12] suggested using a sub-6 GHz band to control a system with multiple APs that operate mainly in the mmWave band.

Multi-band operation can also be interpreted as working in different frequencies within the same frequency band (i.e., working in two mmWave frequencies). For instance, channel bonding and channel aggregation are used in IEEE 802.11ay for multi-band operations [13]. For channel bonding, the UE merges two adjacent 60 GHz channels for data transmission without a guard band. On the other hand, channel aggregation uses two different channels for data transmission.

Another multi-band operation usage is to use one band for control frame exchange and the second band for data transmission exchange. For example, the authors of [14] use two bands that have the same bandwidth for data and control frames, while the authors of [6] use a sub-6 GHz band that has low bandwidth for control frames and a mmWave band that has high bandwidth for data frames, as we adopt in this paper. Dedicating a low-bandwidth band for control frames and a high-bandwidth band for data frames increases the bandwidth utilization efficiency since IEEE 802.11 requires using the lowest modulation coding scheme (MCS) for the control frames, whereas the UEs can use a higher MCS for their data transmission. Combining MuMIMO and IBFD transmission with multi-band operation differentiates our work from [6].

C. Full Duplex Multiuser Multi-Input Multi-Output (MuMIMO)

Integrating IBFD with MuMIMO enables the AP to serve multiple uplink and downlink stations simultaneously. The authors of [22] proposed a spatial grouping strategy for multiuser IBFD. In this protocol, stations are divided into multiple groups such that the uplink stations in one group do not interfere with the downlink stations in another group to mitigate the inter-user interference during the multiuser data transmission. A protocol that uses a full duplex trigger frame to establish a multiuser IBFD connection by using multiple resource units (RU) is proposed in [23]. Similarly, the work in [24] proposed a pairing algorithm that maximizes multiuser full duplex throughput by using multiple RUs. In addition, the authors of [25] proposed a MAC that establishes a second uplink or downlink connection during the idle time of the asymmetric link. In [26], a multiuser MAC protocol was proposed for an asymmetric IBFD configuration. In this protocol, a contention period was proposed where multiple uplink stations send RTS frames to the AP, which increases the protocol overhead.

D. Related Work Summary

In summary, integrating multi-band operation, MuMIMO, and IBFD has not been considered before this work due to the numerous challenges they present. These challenges include support for legacy nodes, the short range of mmWave coverage, the hidden nodes problem, and mitigating the interuser interference, scalability, and station selection. Our work addresses these issues and is an enabler for a multi-band IBFD wireless network.

III. SYSTEM MODELS

We consider a dual-band full-duplex AP that works in sub-6 GHz (i.e., μ Wave) and 60 GHz (i.e., mmWave) bands

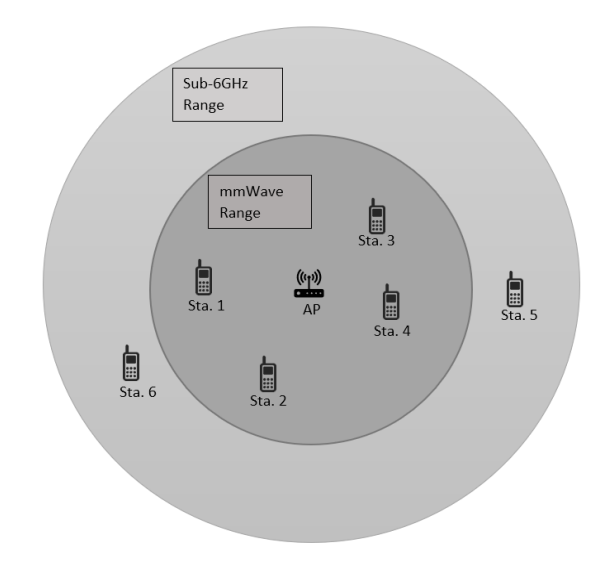


Fig. 1. An example of the system layout. The AP covers two regions: the sub-6 GHz range (light gray) and the mmWave range (Dark gray).

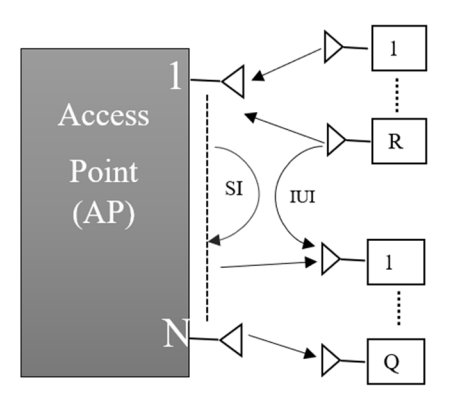


Fig. 2. Sub-6 GHz band system model.

with multiple antennas in each band. Also, we consider M dual-band half-duplex stations with single antennas in both bands at different distances from the AP, as shown in Fig. 1. We now present the system model and state the MAC protocol requirements to support multi-band operation to serve multiple users using a full duplex AP.

A. System Model for Sub-6 GHz Band

In this band, we assume that the AP supports IBFD and has N antennas that are connected to separate radio frequency (RF) chains, which enables the AP to simultaneously serve up to N uplink and N downlink stations. During data transmission in the sub-6 GHz band, the AP serves Q downlink and R uplink stations from the available M stations such that Q+R <= M, Q <= N, and R <= N, as depicted in Fig. 2. At a downlink station q, the resulting received signal, $y_{q-\mu Wave}$, is:

$$y_{q-\mu Wave} = \boldsymbol{h}_{Dq}^{H} \boldsymbol{F}_{D} \boldsymbol{x}_{DQ} + \sum_{r=1}^{R} h_{rq} x_{Ur} + n_{Dq}$$
 (1)

Here, $\pmb{h}_{Dq} \in \mathbb{C}^{N \times 1}$ is the channel between station q and the AP; $\pmb{F}_D \in \mathbb{C}^{N \times Q}$ is the precoding beamforming matrix; $\pmb{x}_{DQ} \in \mathbb{C}^{Q \times 1}$ is the signal from the AP to the downlink

TABLE I NOTATIONS

Symbol	Definition	Symbol	Definition
N	Number of antennas (μWave band).	h_{jk}	The channel between the station k and uplink station j .
Q	Number of downlink stations (µWave band).	x_{uj}	Transmitted signal from station <i>j</i> .
R	Number of uplink stations (µWave band).	n_{Dk}	Received noise at station k.
M	Total number of stations.	σ^2_{Dk}	Noise power at station k .
y _{q-μWave}	Received signal at downlink station q.	$y_{ ext{AP-mmWave}}$	Received signal vector at the AP (mmWave band).
h_{Dq}	Channel between station q and the AP.	$ ho_U$	The average received power from the uplink stations
F_D	μWave precoding beamforming matrix.	W_{BB}	The baseband uplink digital combiner (mmWave band).
x_{DQ}	Downlink signal on the μWave band.	W_{RF}	The analog phase shifter combiner (mmWave band).
h_{rq}	The channel between users r and q .	$oldsymbol{h}_{Uj}$	The uplink channel for station <i>j</i> .
x_{Ur}	Uplink signal from station r	n_{uj}	Received noise at the AP.
n_{Dq}	Received noise at the downlink receiver (µWave band)	H_{SI}	Self-interference channel (mmWave band)
σ^2_{Dq}	Noise power at downlink station q .	σ^2_{Uj}	Noise power for station <i>j</i> .
y _{AP-μWave}	The received signals at the AP (µWave band).	N _{rays}	The number of multipath components
W	Beamforming combiner (µWave band).	$N_{cluster}$	The number of scattering clusters
\boldsymbol{h}_{Ur}	The channel vector between the AP and stations r .	$z_{c,l}$	A complex i.i.d. variable.
G_D	Self-interference channel.	$\alpha(\theta_{c,l})$	Antenna array response vector for AOA.
n_{Ur}	Received noise at the AP.	$\alpha(\mathcal{O}_{c,l})$	Antenna array response vector for AOD.
w_r	Beamforming vector for station r .	R_f	Rician factor.
σ^2_{Ur}	Noise power for station r .	λ_c	Carrier wavelength.
$R_{\mu Wave}$	Total rate at the μWave band.	$R_{\mu Wave}$	Total rate at the mmWave band.
N_T	Number of transmission antennas (mmWave band).	u_{μ}	Combination of uplink stations (µWave band).
N_{T-RF}	Number of transmission RF chains (mmWave band).	D μ	Combination of downlink stations (µWave band).
K	Number of downlink stations (mmWave band).	Um	Combination of uplink stations (mmWave band).
S_K	Number of downlink streams (mmWave band).	Д т	Combination of downlink stations (mmWave band).
N_R	Number of reception antennas (mmWave band).	\mathcal{U}_{RTS}	Uplink contention winners.
N_{R-RF}	Number of reception RF chains (mmWave band).	τ_u	Uplink deficit counter.
J	Number of uplink stations (mmWave band).	τ_d	Downlink deficit counter.
S_J	Number of uplink streams (mmWave band)	$\mathcal{D}\mu_{in}$	The potential downlink stations (µWave band).
y _{k-mmWave}	Received signal at downlink station k.	$\mathcal{D}m_{in}$	The potential downlink stations (mmWave band).
ρ_{Dk}	Average received power from station k.	U m _{RTS}	Uplink contention winners (µWave band).
\boldsymbol{h}_{Dk}	The downlink channel between the AP and station k .	U m _{RTS}	Uplink contention winners (mmWave band).
F	HBF precoding vector.	V	Number of mmWave data transmission segments.
x_{DK}	Transmitted signal vector from the AP (mmWave band).	δ_m	One deficit unit (mmWave band).
ρ_{uj}	Average received power from station <i>j</i> .	δ_{μ}	One deficit unit (µWave band).

stations; h_{rq} is the channel between uplink station r and downlink station q; x_{Ur} is the uplink signal from station r; n_{Dq} is the additive white Gaussian noise (AWGN) with zero mean and unit variance. The resulting signal to interference and noise ratio (SINR) for station q is given by:

$$SINR_{D}\left(q\right) = \frac{\left|\boldsymbol{h}_{Dq}^{H}\boldsymbol{F}_{D}\boldsymbol{x}_{DQ}\right|^{2}}{\left|\sum_{r=1}^{R}h_{rq}\boldsymbol{x}_{Ur}\right|^{2} + \sigma_{Dq}^{2}},$$
(2)

where σ_{Dq}^2 is the noise power. Similarly, the received signal after beamforming, $\mathbf{y}_{AP-\mu Wave} \in \mathbb{C}^{R\times 1}$, at the AP from R uplink stations are:

$$egin{aligned} oldsymbol{y}_{AP-\mu ext{Wave}} &= \sum_{r=1}^R oldsymbol{W}^H oldsymbol{h}_{Ur} x_{Ur} \ &+ oldsymbol{W}^H oldsymbol{G}_D oldsymbol{F}_D oldsymbol{x}_{DO} + oldsymbol{W}^H oldsymbol{n}_{UR}. \end{aligned}$$

Here, $\textbf{\textit{W}} \in \mathbb{C}^{N \times R}$ is the beamforming combiner; $\textbf{\textit{h}}_{Ur} \in \mathbb{C}^{N \times 1}$ is the channel for uplink station r; $\textbf{\textit{G}}_D \in \mathbb{C}^{N \times N}$ is the channel between the antennas of the AP (i.e., self-interference channel); $\textbf{\textit{n}}_{Ur} \in \mathbb{C}^{N \times 1}$ is the AWGN. The resulting SINR for the uplink station r is given by:

$$SINR_{U}(r) = \frac{\left|\boldsymbol{w}_{r}^{H}\boldsymbol{h}_{Ur}\boldsymbol{x}_{Ur}\right|^{2}}{\left|\boldsymbol{w}_{r}^{H}\boldsymbol{G}_{D}\boldsymbol{F}_{D}\boldsymbol{x}_{DQ}\right|^{2} + \sigma_{Ur}^{2}}.$$
 (4)

Here, $\mathbf{w}_r \in \mathbb{C}^{N \times 1}$ is the beamforming vector for the station r such that its elements are equal to the r^{th} row in \mathbf{W}^H ; σ_{Ur}^2 is the noise power for station r.

In the μ Wave band, the channel is modeled as $h=\partial \vartheta$, where ∂ is the path loss between two nodes, and ϑ is a complex independent and identically distributed (i.i.d) random variable with zero mean and unit variance [29]. To enable the IBFD connections, we use the beamforming method in [30] that enables the AP to serve multiuser transmissions and mitigate the self-interference (i.e., the interference that the AP

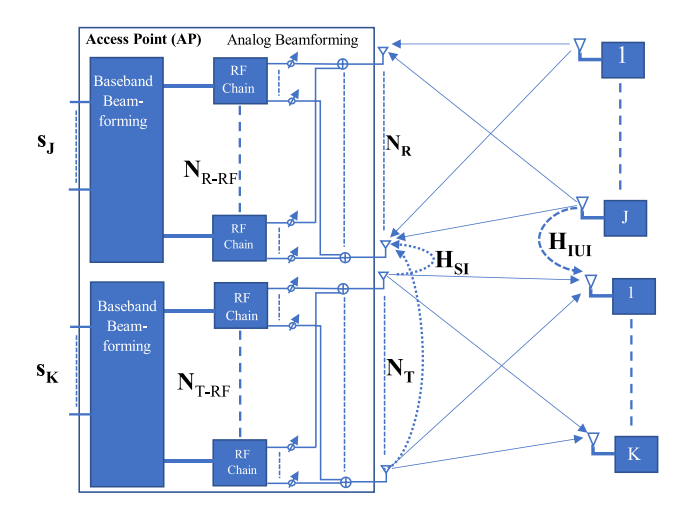


Fig. 3. MmWave system model.

encounter due to the full duplex transmission) and inter-user interference (i.e., the interference that a downlink station encounters form to the concurrent uplink stations' transmission). In addition, we use the IEEE 802.11ax standardized rates ([31] (Table 20-20) that are generated using the average received signal strength indicator (RSSI) and SINR to find the transmission rate of each user. The following equation shows the sum rate of the sub-6 GHz band for a set of $\mathcal{U}\mu$ and $\mathcal{D}\mu$ uplink and downlink stations, respectively.

$$R_{\mu Wave} = \sum_{u\mu \in \mathcal{U}\mu} Rate\left(SINR_{u\mu}, RSSI_{u\mu}\right) + \sum_{d\mu \in \mathcal{D}\mu} Rate\left(SINR_{d\mu}, RSSI_{d\mu}\right). \tag{5}$$

B. System Model for mmWave Band

The AP's mmWave transceivers have N_T and N_R transmission and reception antennas, respectively. The AP transmits data to K stations by generating S_K streams that feed N_{T-RF} RF chains and are connected to N_T transmission antennas such that $N_T \gg N_{T-RF} \geq K{=}S_K$. Also, the AP has N_R reception antennas, where N_{R-RF} RF chains are connected to a baseband decoder that yields S_J streams such that $N_R \gg N_{R-RF} \geq J = S_J$, as shown in Fig. 3. In addition, we assume the AP uses hybrid beamforming (HBF) for precoding the transmitted signals and decoding the received signals [32]. The received signal, $y_{k-mmWave}$, at a downlink station k is represented by:

$$y_{k-mmWave} = \sqrt{\rho_{Dk}} \boldsymbol{h}_{Dk}^{H} \boldsymbol{F}^{H} \boldsymbol{x}_{DK} + \sum_{j=1}^{J} \sqrt{\rho_{uj}} h_{jk} x_{Uj} + n_{Dk}.$$
 (6)

Here, ρ_{Dk} is the average received power; $\boldsymbol{h}_{Dk} \in \mathbb{C}^{NT \times 1}$ is the downlink channel between the AP and station k; $\boldsymbol{F} \in \mathbb{C}^{NT-RF \times NT}$ is the HBF precoding vector; $\boldsymbol{x}_{DK} \in \mathbb{C}^{NT-RF \times 1}$ is the transmitted signal vector from the AP; ρ_{uj} is the average received power from station j; h_{jk} is the channel between the station k and uplink station k; k is the transmitted signal from station k; k is the AWGN with

zero mean and unit variance. Hence, the resulting SINR for downlink station k with σ_{Dk}^2 noise power is:

$$SINR_{D-mmWave}(k) = \frac{\left|\sqrt{\rho_{Dk}} \boldsymbol{h}_{Dk}^{H} \boldsymbol{F}^{H} \boldsymbol{x}_{DK}\right|^{2}}{\left|\sum_{j=1}^{J} \sqrt{\rho_{uj}} \boldsymbol{h}_{jk}^{Xuj}\right|^{2} + \sigma_{Dk}^{2}}. (7)$$

On the other hand, the received signal after hybrid beamforming, $y_{AP-mmWave} \in \mathbb{C}^{J \times 1}$, at the AP from J uplink stations is given by:

$$\mathbf{y}_{AP-mmWave} = \sum_{j=1}^{J} \sqrt{\rho_{U}} \mathbf{W}_{BB}^{H} \mathbf{W}_{RF} \mathbf{h}_{Uj} x_{j}$$

$$+ \mathbf{W}_{BB}^{H} \mathbf{W}_{RF} \mathbf{H}_{SI} \mathbf{F}^{H} \mathbf{x}_{DK}$$

$$+ \mathbf{W}_{BB}^{H} \mathbf{W}_{RF} \mathbf{n}_{UJ}.$$
 (8)

Here, ρ_U is the average received power from the uplink stations; $\mathbf{W}_{BB} \in \mathbb{C}^{NR-RF \times J}$ is the baseband uplink digital combiner; $\mathbf{W}_{RF} \in \mathbb{C}^{NR-RF \times 1}$ is the analog phase shifter combiner [33]; $\mathbf{h}_{Uj} \in \mathbb{C}^{NR \times 1}$ is the uplink channel for station j; $\mathbf{n}_{uj} \in \mathbb{C}^{N \times 1}$ is the AWGN vector with zero mean and unit variance; $\mathbf{H}_{SI} \in \mathbb{C}^{NR \times NT}$ is the self-interference channel. The resulting uplink SINR for station j is given by:

$$SINR_{U-mmWave}(j) = \frac{\left|\sqrt{\rho}_{Uj} \boldsymbol{w}_{BB}^{H} \boldsymbol{W}_{RF} \boldsymbol{h}_{Uj} \boldsymbol{x}_{Uj}\right|^{2}}{\left|\boldsymbol{w}_{BB}^{H} \boldsymbol{W}_{RF} \boldsymbol{H}_{SI} \boldsymbol{F}^{H} \boldsymbol{x}_{DK}\right|^{2} + \sigma_{Uj}^{2}},$$
(9)

where $\mathbf{w}_{BB} \in \mathbb{C}^{NR-RF \times 1}$ is the baseband beamforming vector for the station j such that its elements are equal to the j^{th} row in \mathbf{W}_{BB}^{H} , and σ_{Uj}^{2} is the noise power for station j. We assume the AP has a uniform linear antenna array (ULA) configuration that results in a channel model with N_{R}

(ULA) configuration that results in a channel model with N_R and N_T antennas at its receiver and transmitter, $\mathbf{H} \in \mathbb{C}^{NR \times NT}$, as follows [34]:

$$\boldsymbol{H} = \sqrt[2]{\frac{N_T N_R}{N_{rays} N_{Cluster}}}$$

$$\sum_{c=1}^{N_{Cluster}} \sum_{l=1}^{N_{rays}} z_{c,l} \boldsymbol{a}_r \left(\theta_{c,l}\right) \boldsymbol{a}_t^H \left(\emptyset_{c,l}\right). \tag{10}$$

Here, N_{rays} is the number of multipath components; $N_{cluster}$ is the number of scattering clusters; $z_{c,l}$ is a complex i.i.d random variable with zero mean and unit variance that represents the channel gain at path l; $\emptyset_{c,l}$ is the transmitter angle of departure (AOD); $\theta_{c,l}$ is the receiver angle of arrival (AOA); $\alpha(\theta_{c,l}) \in \mathbb{C}^{NR \times 1}$ and $\alpha(\emptyset_{c,l}) \in \mathbb{C}^{NR \times 1}$ are the antenna array response vectors for AOA and AOD, respectively, defined in [32]. In addition, we assume the self-interference channel $\mathbf{H}_{SI} \in \mathbb{C}^{NR \times NT}$ consists of a near-field line of sight (LOS) and far-field non-line of sight (NLOS) components:

$$\boldsymbol{H}_{SI} = \sqrt{\frac{R_f}{1 + R_f}} \boldsymbol{H}_{LOS} + \sqrt{\frac{1}{1 + R_f}} \boldsymbol{H}_{NLOS}, \quad (11)$$

where R_f is the Rician factor. The element $[H_{LOS}]_{mn}$, in the m^{th} row and n^{th} column of the LOS channel matrix,

is modeled by [35]:

$$[H_{LOS}]_{mn} = \frac{\beta}{r_{mn}} \exp\left(-j2\pi \frac{r_{mn}}{\lambda_c}\right),\tag{12}$$

where β is a normalization factor such that $E[|H_{SI}||_F^2] = N_T N_R$, r_{mn} is the distance between the m^{th} and n^{th} element of the transmit array, and λ_c is the carrier wavelength. We obtain H_{NLOS} using (9). Finally, we use the IEEE 802.11ay standardized method for rate adaptation [36] (Table 28-68) that is based on RSSI and SINR that can be found after acquiring the channels of the participant stations in an active mmWave data transmission. The mmWave sum rate of a set of $\mathcal{U}m$ and $\mathcal{D}m$ uplink and downlink stations is as follows.

$$R_{mmWave} = \sum_{um \in Um} Rate\left(SINR_{um}, RSSI_{um}\right) + \sum_{dm \in Dm} Rate\left(SINR_{dm}, RSSI_{dm}\right). \quad (13)$$

IV. MB-FDMAC PROTOCOL

The system under study poses many challenges for the full-duplex AP. First, the AP must acquire updated channel state information (CSI) from the uplink and downlink stations to determine the beamforming coefficients, which enable the AP to send and receive data from multiple stations. Second, the uplink stations' concurrent transmissions with the AP produce inter-user interference (IUI) at the downlink stations that must be addressed to ensure a successful downlink transmission. The work in [37] provides an IUI mitigation technique that requires knowledge at the AP of the combined interference levels that each downlink station encounters from the uplink stations. The AP's final challenge is to select stations for uplink and downlink transmission in each band. The selection of users (i.e., sets $\mathcal U$ and $\mathcal D$) determines the system performance achieved and will be addressed in the sequel.

To resolve the previous challenges, we propose the MB-FDMAC protocol that enables the full duplex AP to serve multiple stations simultaneously. Furthermore, MB-FDMAC is based on the IEEE 802.11 DCF and supports legacy nodes. In MB-FDMAC, the sub-6 GHz band timeline is divided into segments that control the operation of the mmWave band and exchange data from sub-6 GHz stations. In addition, the mmWave band timeline is divided into multiple data exchange segments, such that each data segment depends on the previous sub-6 GHz control segment. Fig. 4 shows the timeline of MB-FDMAC in both bands. In the following subsections, we explain in detail the operation of MB-FDMAC on each band.

A. MB-FDMAC Sub-6 GHz Band Frame Structure

The stations associated with the AP can either support both bands or only the sub-6 GHz bands. Hence, the MB-FDMAC frame structure in the sub-6 GHz bands is adaptive to the type of the associated stations with the AP. Therefore, first, we discuss the frame structure of MB-FDMAC with all associated stations within the mmWave band range. Then, we show changes in the MB-FMDAC frame structure with

if there is any station that outside the mmWave range and support the sub-6 GHz band.

In MB-FDMAC, the sub-6 GHz band has three stages when all the associated stations with the AP are in the mmWave range. In the first stage, the AP broadcasts a beacon frame (AP Beacon) that notifies the stations to begin contending for uplink transmission and the contention duration. In the second stage, each uplink station selects a random backoff counter from $[0, 2^{\rm CW}]$, where CW is the station contention window ranging from 4 to 10. Then, stations reduce their backoff counters after a distributed inter-frame space (DIFS). After that, stations sense the medium and send a request to send (RTS) frame to the AP if the medium is idle upon the expiration of their backoff counter. Otherwise, the stations wait until the medium becomes idle. A collision occurs when two stations send an RTS simultaneously, and we analyze its effects in Section VI-C.4. The length of the contention stage, $T_{Cont.}$, is:

$$T_{Cont.} = T_{SIFS} + T_{RTS} * \Delta_{cont.}$$
 (14)

Here, $\Delta_{cont.}$ is a scalar that determines the maximum number of potential uplink stations; $T_{\rm SIFS}$ is the short inter-frame space (SIFS); $T_{\rm RTS}$ is the duration for sending an RTS frame using the lowest modulation rate (i.e., MCS0 rate).

In the final sub-6 GHz stage, the AP sends a CTS to the selected uplink stations. The length of this stage, T_{CTS} , is:

$$T_{CTS} = \frac{(14+6*J)*8}{MCS0\ rate},$$
 (15)

where J is the number of the uplink stations in the mmWave band range. The CTS frame uses 14 bytes of overhead (control bits) and 6 bytes for the address of each uplink station. By the end of this stage, MB-FDMAC pursues the data transmission on the mmWave band, as explained in the next subsection. Then, the AP starts the same procedure in the next controlling segment. However, if there is any station that is outside the range of the mmWave band but within the range of the sub-6 GHz band, the AP replaces the CTS frame in a control segment with a clear and request to send (C/RTS) frame. The C/RTS frame serves as a CTS frame for all the uplink stations (sub-6 GHz and mmWave) and an RTS frame for sub-6 GHz stations. The length of this stage, T_{C/RTS}, is:

$$T_{C/RTS} = \frac{14 + 6 * (J + R + Q)}{MCS0 \ rate}$$
 (16)

Here, R and Q are the numbers of uplink and downlink stations, respectively, that are in the sub-6 GHz band range. Similar to the CTS frame, the C/RTS uses 14 bytes of overhead (control bits) and 6 bytes for the address for each uplink station.

In addition, MB-FDMAC introduces three more sub-6 GHz stages to accommodate the sub-6 GHz stations. The first stage is the sub-6 GHz CTS stage. In this stage, the sub-6 GHz downlink stations send a CTS frame to the AP after receiving the C/RTS frame. The CTS-6GHz frame contains the interference level that the station encounters from the other uplink stations that operate only in the sub-6 GHz band. The duration,

AP	AP Beacon					C/RT 1,4,5		Data to 6	ACK to 5		
	20000					/6*					
	Data transmis	ssion fro	m the pr	evious p	eriod			Interfer manageme Beamfor	nt and	Data to 2,3	ACK to 1,4
Sta.1		RTS									
										Data to AP	
Sta. 2			RTS								
											ACK to AP
Sta. 3			RTS								
											ACK to AP
Sta. 4				RTS							
										Data to AP	
Sta. 5*					RTS			Data to AP			
Sta. 6*							CTS		ACK to AP		
	2		~				veno.		a .		
μWave Band (Light Rows)	Beacon Stage	e Contention Stage				CTS tage	μWave data Stage		μWave segment (n+1)		
	μWave segment (n)										
MmWave Band (Dark						Beamforming	stage	mmWave Data stage	Ack Stage		
Rows)						mmWave segment (n)					

Fig. 4. A timeline example for MB-FDMAC protocol. Here, stations 5 and 6 support only the sub-6 GHz band, while other stations support both bands. We assume that the AP has $N_{\rm T-RF}=N_{\rm R-RF}=N=2$, which means the AP can only perform two concurrent full duplex transmissions in any band. In this example, the AP successfully received three RTS frames from stations 1, 4, and 5, while the RTS frames from stations 2 and 3 collided and were not received.

 $T_{CTS-6GHz}$, of this stage is:

$$T_{CTS-6GHz} = \left(\frac{16 * 8}{MCS0 \ rate}\right) * Q,\tag{17}$$

where the station uses two bytes to report the interference in addition to the 14 overhead bytes. Also, it is worth mentioning that the AP uses the received control frames (RTS and CTS frames) to estimate the required channels for beamforming. After that, the AP and the uplink stations start sending their data frames during the second additional stage. The duration of this stage, $T_{\rm D-6GHz}$, is fixed by the network administrator. The final stage is the Sub-6 GHz ACK stage. During this stage, the AP sends an ACK to all the uplink stations upon receiving all the uplink data frames. Simultaneously, the downlink stations send an ACK to the AP for the received downlink data frames. Fig. 5 shows the components of the control frames in the sub-6 GHz.

B. MB-FDMAC MmWave Band Frame Structure

In IEEE802.11ay, the mmWave timeline is divided into a beacon header interval (BHI) and a data transfer interval (DTI) [13]. Without loss of generality, we assume that MB-FDMAC operates in the DTI after the BHI is completed.

The mmWave band in MB-FDMAC consists of three stages. The first stage is the mmWave beamforming stage, which

	FCS 4 Bytes						
(a)							
Duration 2 Bytes	AP Address 6 bytes	Transmitter address 6 bytes	FCS 4 Bytes				
(b)							
Duration 2 Bytes	AP Address 6 Bytes	Stations addresses (J+R+Q)*6 Bytes	FCS 4 Bytes				
(c)							
Duration 2 Bytes	AP Address 6 Bytes	Encountered Interference 2 Bytes	FCS 4 Bytes				
(d)							
Duration 2 Bytes	Tra	FCS 4 Bytes					
	Duration 2 Bytes Duration 2 Bytes Duration	Duration 2 Bytes Address 6 bytes Duration AP Address 6 Bytes Duration Train	Duration 2 Bytes Address 6 bytes (b) Duration 2 Bytes Address 6 bytes (b) Duration 2 Bytes Address 6 Bytes (c) Duration 2 Bytes Address 6 Bytes (c) Duration 2 Bytes Address 6 Bytes (c) Duration 2 Bytes Address Interference 2 Bytes (d) Duration Transmitter Address				

Fig. 5. Sub-6 GHz band Frame structure: (a) AP beacon, (b) RTS frame, (c) R/CTS frame, (d) sub-6 GHz CTS frame, (e) sub-6 GHz ACK. Note figure size does not reflect the actual frame size.

starts after the end of the C/RTS (or CTS with all stations within mmWave range) transmission in the sub-6 GHz band. In this stage, the AP collects the required data for HBF by

Frame	Duration	AP	Stations addresses	FCS				
Control	2 Bytes	address	(J+K) *6 Bytes	4 Bytes				
2 Bytes	-	6 bytes						
	(a)							
Frame	Duration	AP	Transmitter address	FCS				
Control	2 Bytes	address	6 Bytes	4 Bytes				
2 Bytes		6 Bytes						
	(b)							
Frame	Duration	AP	Encountered	FCS				
Control	2 Bytes	address	Interference	4 Bytes				
2 Bytes		6 Bytes	2 Bytes	·				
	(c)							
Frame	Duration	Transmitter Address		FCS				
Control	2 Bytes	6 Bytes		4 Bytes				
2 Bytes	_		-					
(d)								

Fig. 6. MmWave band frame structure: a) AP polling frame, (b) uplink reply frame, (c) downlink reply frame, (d) and mmWave ACK frame. Note figure size does not reflect the actual frame size.

sending a polling frame (PF) to the uplink contention winners and the selected downlink stations. Then, each uplink station sequentially sends an uplink reply frame (URF) to the AP. The URF enables the AP to acquire the channel of each uplink station. Next, downlink stations sequentially send a downlink reply frame (DRF) to the AP. The DRF contains the combined level of interference that a downlink station encounters from the uplink stations during their URF transmission. Also, the AP acquires the channel for each downlink station from the received DRF using channel reciprocity. The length of the beamforming stage, T_{BF} , is:

$$T_{BF} = (T_{mSlot} + T_{mSIFS}) * (K + J + 1).$$
 (18)

Here, $T_{\rm mSlot}$ and $T_{\rm mSIFS}$ are the slot time and SIFS in the mmWave band. Then, the AP starts sending data to the downlink stations in the second stage while receiving data from the uplink stations. The length of this stage, T_D , is:

$$T_D = T_{AP-beacon} + T_C - T_{BF} - T_{ACK}.$$
 (19)

Here, $T_{AP-Beacon}$ is the time to transmit the AP beacon in the sub-6 GHz band; T_{ACK} is the time to send an ACK frame in the mmWave band. In the final mmWave band stage, the AP sends a block ACK frame to the uplink stations, and the downlink stations send their ACK frames to the AP. During this stage, the uplink stations have already started contending for the uplink transmission in the sub-6 GHz band, which justifies using the mmWave band to send the ACK frames. Fig. 6 shows the components of the aforementioned control frames in the mmWave band.

C. Leveraging the Bandwidth of MmWave

MB-FDMAC offers a feature that improves the utilization of the large instantaneous mmWave bandwidth by dividing T_D in (19) into multiple segments, such that:

$$T_D = V(T_0 + T_{mRIFS}), (20)$$

where V is the number of segments; T_0 is the duration of each segment; T_{mRIFS} is the reduced inter-space frame space (RIFS);

This feature reduces the idle time in the mmWave data transmission stage if there is no more data to send during this stage (either by the stations to the AP or vice versa), which enables the AP to serve different stations in the next T_0 . In addition, this feature reduces the number of rejected stations that send an RTS frame to the AP due to the lack of an available uplink stream. To illustrate, the AP will be able to serve $2N_{T-RF}$ uplink stations with $T_0=2$ instead of only N_{T-RF} uplink stations with $T_0=1$. However, the benefits of this modification in the data transmission stage come with a cost of an additional overhead that MB-FDMAC encounters in the mmWave band, as follows. First, the length of the beamforming stage (i.e., T_{BF}) increases with the increased number of selected stations for mmWave transmission. Second, RIFS is required between each T_0 . Finally, the length of the ACK stage increases with the increased number of selected stations since the AP can only receive N_{R-RF} ACK frames at any given time. Nevertheless, the duration of the additional overhead is marginal compared to the length of the data stage, making this multiplexing worthy.

V. Multi-Band Joint Station Selection Algorithm

Station selection is a major challenge in the design of MB-FDMAC due to the following constraints. (i.) The number of selected stations on each band cannot exceed the number of RF chains in that band. (ii.) The AP can only select uplink stations from stations that send RTS successfully during the contention stage, limiting the availability of uplink stations. (iii.) The AP can only select a station as an uplink or downlink station since these stations operate in the half-duplex mode. (iv.) The AP must select the serving band for each station based on the transmit range in the selected band. In addition, station selection affects the sum rate of the system since the uplink stations interfere with the downlink signals, thereby affecting the SINR, as shown in (5) and (13).

One easy solution for the AP is to select uplink stations on a first-come, first-serve basis. With this solution, the AP selects the first N_{R-RF} contention winners (\mathcal{U}_{RTS}) that support the mmWave band as uplink stations on this band. In addition, if there is any contention winner that does not support the mmWave band, the AP selects the first N stations from those sub-6 GHz contention winners as uplink stations for the sub-6 GHz band. Then, the AP randomly selects up to N and N_{T-RF} downlink stations for the sub-6 GHz and mmWave bands, respectively. This approach, however, might create imbalanced uplink and downlink traffic and cause an unfair allocation of resources. Also, non-selected stations may suffer from data starvation, resulting in a dropped data packet or outdated packet transmission.

To solve the aforementioned problem, we introduce a multi-band joint station selection (MB-JSS) algorithm that enables the AP jointly to select uplink and downlink stations on both bands. MB-JSS is based on the deficit round-robin algorithm [38] to ensure uplink and downlink fairness among the stations. Consequently, MB-JSS considers in its selection decision the time the stations spend on uplink and downlink traffic to ensure that the stations receive a fair time for transmitting and receiving data. MB-JSS assigns an uplink

 (τ_u) and downlink (τ_d) deficit counter (measured in seconds) for each station to measure their traffic. These deficits serve as a starvation indicator, meaning that the higher the station's deficit (uplink or downlink), the less time this station has been served. Furthermore, these deficits are used to track the uplink and downlink traffic of each station that MB-JSS leverages to balance the uplink and downlink throughput of each station. These deficits are initialized to zero for any new station that joins the network. This initialization process ensures that the old station deficits are considered in the selection process by the MB-JSS.

The inputs of the MB-JSS algorithm are the uplink and downlink deficits, sub-6 GHz band potential downlink stations $(\mathcal{D}\mu_{in})$, mmWave band potential downlink stations $(\mathcal{D}m_{in})$, and uplink contention winners (\mathcal{U}_{RTS}) that are divided into two groups: (i.) stations that support mmWave $(\mathcal{U}m_{RTS})$ and (ii.) stations that support μ Wave band only $(\mathcal{U}\mu_{RTS})$. In addition, MB-JSS requires the number of antennas in the sub-6 GHz band (N) and the number of transmitting and receiving streams at the mmWave band (i.e., N_{T-RF} and N_{R-RF} ; for simplicity, we assume $N_{T-RF} = N_{R-RF} = Nm$).

The process of MB-JSS for stations that support mmWave is as follows. The AP considers 2Nm stations as potential downlink stations (' $\mathcal{D}m_{\rm in}$) that have the highest downlink deficit among other stations within the network. Then, the AP sorts the stations in Um_{RTS} based on their uplink deficit counter. After that, the AP considers two groups of stations as initially selected. The first group consists of Nm (or less depending on the number of stations in $\mathcal{U}m_{RTS}$) uplink candidates ($\mathcal{U}m$) that have the highest uplink deficits, and the second group consists of 2Nm potential downlink stations ($\mathcal{D}m$) from $\mathcal{D}m_{in}$ that have the highest downlink deficits. Since the stations are half-duplex stations, the AP declares the Um and Dm stations as uplink and downlink stations if and only if there are no common stations between those two groups. Otherwise, the AP starts revising the considered stations in both groups to ensure balancing the uplink and downlink throughput of each station within the network. Therefore, the AP compares the uplink and downlink deficits of the common stations in those groups. Accordingly, the AP removes any uplink candidate from $\mathcal{U}m_{RTS}$ with a downlink deficit that is higher than the uplink deficit and removes any potential downlink station from $\mathcal{D}m_{in}$ with a downlink deficit that is less than the uplink deficit. Then, the AP repeats the process by creating the two groups of uplink and downlink stations with remaining stations until convergence, which only occurs if there are no overlapping stations in Um and Dm. Finally, after the station selection, the MB-JSS algorithm updates the uplink and downlink deficits by subtracting the amount of mmWave network usage - that we define as δ_m - from the deficits (i.e., τ_u and τ_d) of the selected stations, which ensures that the non-selected stations have a higher priority in the next round. It is worth noting that MB-JSS accommodates the data stage segmenting feature in MB-FDMAC by repeating the aforementioned mmWave selection process at each segment.

During the mmWave selection process, MB-JSS also starts selecting stations that only support sub-6 GHz, which only occurs if there is any station that supports only the sub-6 GHz

TABLE II SIMULATION PARAMETERS

μWave	Value	mmWave	Value
Parameter		Parameter	
Slot time	9 μs	Slot time	5 μs
SIFS	16 μs	SIFS	3 μs
DIFS	34 μs	DIFS	13 µs
TXOP	85 μSec	TXOP	170 µs
Frame	34 Bytes	Frame	60 Bytes
Overhead		Overhead	
Bandwidth	20 MHz	Bandwidth	2.16 GHz

band within the network. The sub-6 GHz band selection process is similar to the mmWave band selection process with the following changes. First, MB-JSS sets the number of potential downlink stations ($\mathcal{D}\mu_{\rm in}$) in the sub-6 GHz band to 2N instead of 2Nm. Also, the second group created by the AP in the sub-6GHz band consists of up to N contention winners ($\mathcal{U}\mu_{RTS}$). Then, the AP finalized the selection process in the sub-6 GHz band with a similar process used in the mmWave selection process.

The final outputs of MB-JSS are the mmWave selected uplink stations (Um), the mmWave selected downlink stations (Dm), the μ Wave selected uplink stations $(U\mu)$, the μ Wave selected downlink stations $(D\mu)$, and updated uplink and downlink deficits. Fig. 7 shows the complete steps of the MB-JSS algorithm.

VI. PERFORMANCE EVALUATION

We conduct extensive simulations of MB-FDMAC by using MATLAB. In these simulations, the AP is placed at the center of a 15m-by-15m area. In addition, the stations are randomly placed around the AP. The simulation result represents the average result of twenty different station placements. Furthermore, we assume all stations, including the AP, are fully backlogged (i.e., always have data to send), making the traffic always busy in the data transmission stage. Furthermore, we set the downlink and the uplink maximum transmission power to 27 dBm and 20 dBm, respectively. We assume that the AP supports four active uplink and downlink streams in both bands (i.e., $N_{T-RF} = N_{R-RF} = N = 4$). Finally, we use the rate adaption scheme defined in Table 28-68 in [36] for mmWave and Table 20-20 in ([31] for sub-6 GHz. Table II shows the rest of the parameters used in the simulation.

A. Throughput Comparison

In this subsection, we compare the performance of MB-FDMAC with the following state-of-the-art multiuser mmWave MAC protocols that support up to four streams simultaneously:

FDMUMAC [26]: FDMUMAC is an IBFD MAC protocol that simultaneously serves multiple uplink and downlink stations. In this protocol, the AP collects the

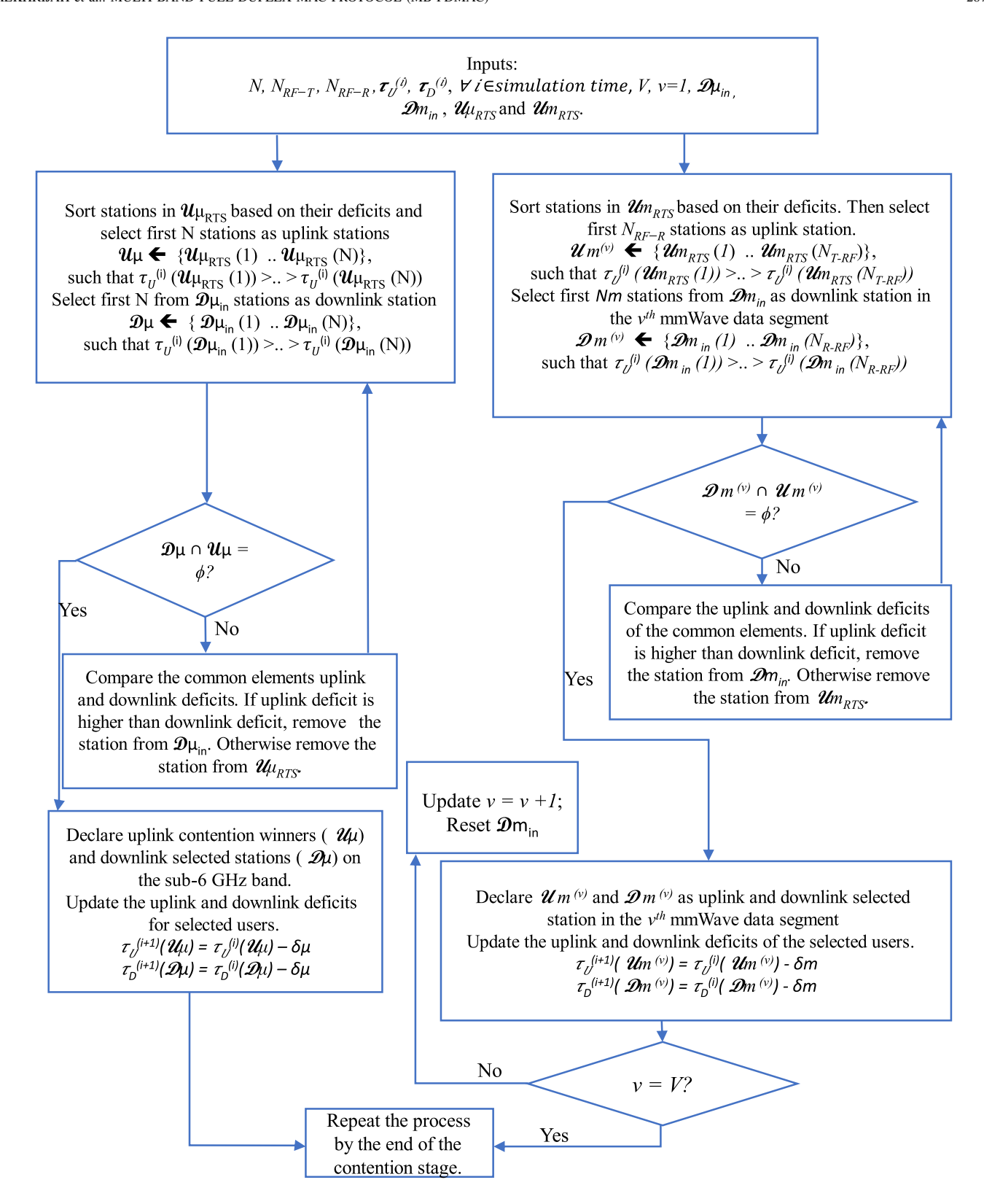


Fig. 7. Flowchart for MB-JSS algorithm. The right side shows the mmWave band selection procedure while the left side shows the sub-6 GHz band selection procedure. The process of MB-JSS starts by the end of the contention stage.

interference and acquires the perfect channel by using the control frames to perform a full duplex connection at the AP and mitigate the inter-user interference at downlink stations to support uplink and downlink streams simultaneously. PDVC-MAC [39]: In this protocol, the AP uses the knowledge of the channel perfectly and the interference levels that downlink stations encounter to mitigate interference. Then, the AP places the stations in multiple groups based on the collected information to avoid

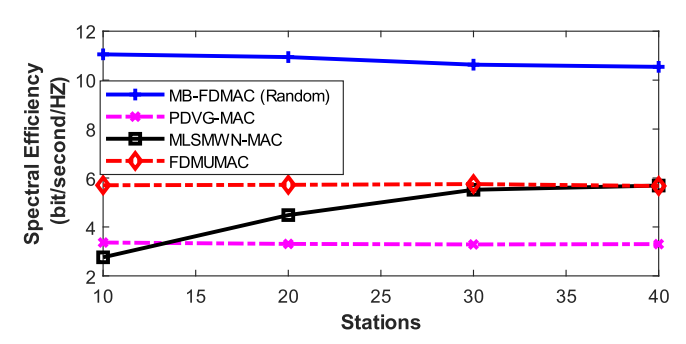


Fig. 8. MB-FDMAC throughput compared with FDMUMAC, PDVC-MAC, and MLSMWN-MAC with respect to the number of stations.

inter-user interference, which increases the throughput for the mmWave multiuser transmission.

 MLSMWN-MAC [40]: This protocol is based on the IEEE 802.11 DCF and utilizes time and frequency multiplexing for the control frame. These control frames are also used to acquire the channels that are then utilized for beamforming. Also, this protocol assumes there is no overlapping between the selected stations, removing the effect of inter-user interference.

However, these works use only a single frequency band. To ensure a fair comparison, we use the spectral efficiency (i.e., bits/sec/Hz) for performance comparison since the utilized bandwidth by MB-FDMAC is 2.18 GHz (2.16 GHz in mmWave band and 20 MHz in the sub-6 GHz band) and utilized bandwidth by other references is 2.16 GHz (only mmWave band). Also, we set the station selection to be at random in MB-FDMAC since the other protocol did not consider fairness in their design.

Fig. 8 shows that MB-FDMAC increases the spectral efficiency by an average of 325%, 234%, and 189% compared with PDVC-MAC, MLSMWN-MAC, and FDMUMAC, respectively. The primary reason for this increase is using IBFD for data transmission compared with the first protocols. Nevertheless, MB-FDMAC spectral efficiency outperforms FDMUMAC significantly, which uses a full duplex AP since the proposed protocol removes the overhead (i.e., control frames) in the mmWave band.

B. Evaluation of MB-FDMAC

We use the following four metrics to compare the performance of the selection methods: (i.) throughput, (ii.) average packet delay, (iii.) downlink temporal fairness, and (iv.) uplink temporal fairness. Here, the throughput is measured as the sum rate of all stations at the end of the simulation. To quantify delay, we define packet delay as the time between starting to contend for uplink transmission to the time of ACK reception. Finally, we use Jain's fairness index [41] to measure the overall fairness of the system. To evaluate MB-FDMAC, we define three selections schemes:

 Random: The AP serves the first Nm uplink contention winners as uplink stations on each band. Then, it randomly selects Nm stations for downlink transmission.
 We set the random method as a benchmark for our simulation because the AP does not consume any computing resources for selecting the stations.

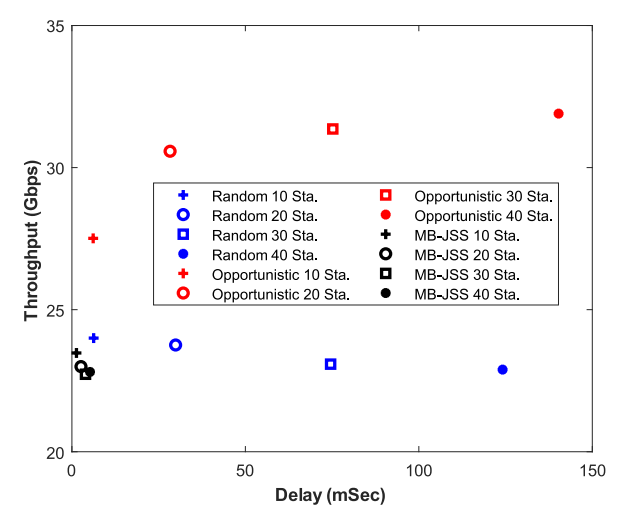


Fig. 9. Throughput (Mbps) versus the delay (mSec) of the Random, Opportunistic and MB-JSS schemes with different numbers of stations.

- Opportunistic: The AP selects a combination of uplink stations from the uplink contention winners and downlink stations other than selected uplink stations that maximize the throughput - assuming the AP has full knowledge of all the channels. Therefore, the throughput of this scheme serves as the performance upper bound.
- MB-JSS: The AP follows the MB-JSS algorithm to select uplink and downlink stations.

1) Throughput: Fig. 9 shows the saturation throughput versus delay for the three previously mentioned selection methods with a different number of stations. We observe, as expected, that the opportunistic scheme achieves the highest throughput since we assume that this selection scheme maximizes the overall throughput without any additional overhead, which sets the performance upper bound. Nevertheless, the Opportunistic scheme is a non-practical scheme compared to other methods since it requires full knowledge of all channels. Also, the opportunistic throughput gains come at the cost of higher average packet delay and lack of fairness, which we show in thescheme.ng subsection. On the other hand, with the practical selection scheme (i.e., Random and MB-JSS), we observe approximately a 24% reduction in throughput with the Random and MB-JSS schemes compared with the opportunistic scheme. In general, the throughput reduction of those two schemes compared with opportunistic scheme comes the massive difference between the transmission rates of difference MCS in the IEEE802.11ay, where the average between two MCS transmission rate is about 15%. In addition, the reduction in throughput for the Random scheme comes from the randomness in selecting the stations without any consideration for the conditions for their channels. Also, the MB-JSS throughput reduction comes from considering the network fairness to select the stations, which also explains the 1.8% throughput reduction compared with the Random scheme.

2) Delay: Reducing the average packet delay is critical for time-sensitive applications. Fig. 9 shows that the MB-JSS scheme significantly lowers the average packet delays than the Random and Opportunistic schemes. In particular, the

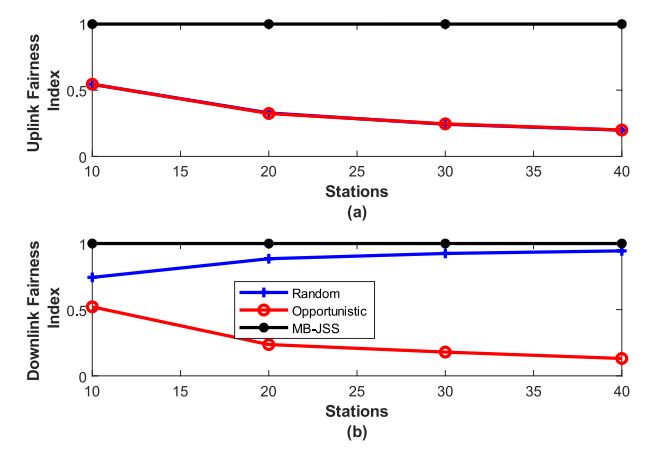


Fig. 10. Fairness versus number of stations. (a) Uplink fairness (b) Downlink fairness. Note the uplink fairness of the Random and Opportunistic schemes overlap.

average delay of the MB-JSS scheme is 94.4% and 94.8% lower compared with the Random and Opportunistic schemes, respectively. Furthermore, these delay reductions increase with the increasing number of stations. MB-JSS's clear reduction in the delay is the result of ensuring all stations have a fair chance to transmit their data, improving the diversity in selecting the stations.

3) Fairness: Fig. 10 shows that the temporal fairness of the MB-JSS scheme significantly outperforms other selection methods. The average uplink and downlink temporal fairness gains of the MB-JSS scheme are 204% and 14.1% compared with the Random scheme. Also, the MB-JSS scheme achieves an uplink and downlink temporal fairness gain of 204% and 274% compared with the opportunistic scheme. These fairness gains increase with the increasing number of stations. For instance, the fairness of MB-JSS with 40 stations outperforms the Random and opportunistic scheme by more than 400% in the uplink temporal fairness. The aforementioned gains over the opportunistic scheme are because the latter ignores the low-rate stations from the station selection. Also, these gains over the Random scheme come from the joint decision in selecting uplink and downlink stations by MB-JSS.

C. Study of MB-FDMAC Parameters

We now present an empirical study on the effect of varying several MB-FDMAC parameters, including the length of contention stage, transmission type (full duplex or half duplex), the accuracy of channel estimation, and collisions. In addition, we study dual-band operation in cooperative and non-cooperative modes.

1) Effect of Contention Stage Length: The contention length $\Delta_{\rm cont.}$ (defined in Section IV-A) plays a critical role in determining the maximum number of uplink stations and the length of the transmission stage in the mmWave band. Fig. 11(a) shows the throughput and average packet delay as a function of contention length for twenty stations. The results show that the throughput increases with an increase in the contention length. This increase comes from (i.) an increase in the overall number of uplink stations that win the contention, (ii.) the overall reduction in time spent on the beamforming construction stage, and (iii.) the increase

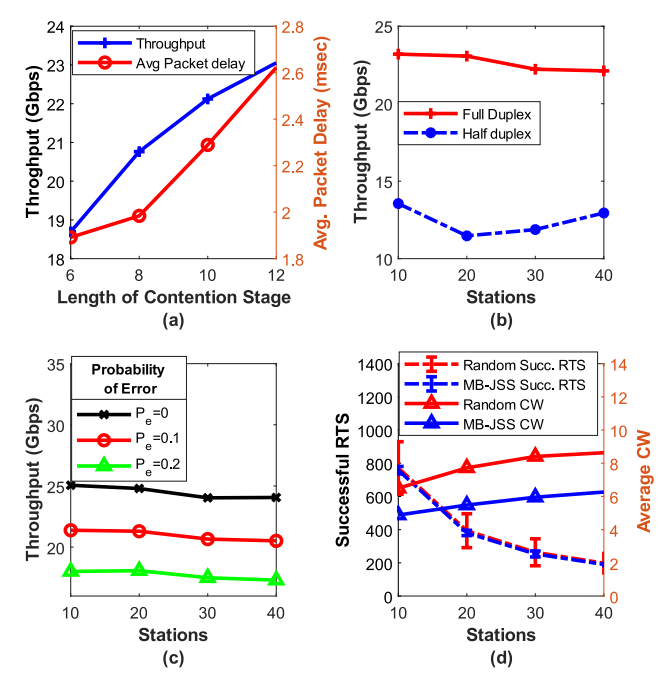


Fig. 11. Simulation results: (a) Throughput and average packet delay Vs. contention stage. (b) Full duplex Vs. half duplex throughput. (c) Throughput under different channel probability of errors. (d) Successful RTS transmission, RTS lost packets and average CW size for MB-JSS and Random methods.

in the data transmission time in the mmWave band for the backlogged stations. Since $\Delta_{\rm cont.}$ determines the transmission stage length, non-participants in the transmission stage will suffer from high packet delay. Fig. 11(a) also shows that the average packet delay increases with an increase in the length of the contention stage for two reasons. The first reason is the increase in waiting time for the C/RTS frame. The second reason is the limited resource availability at the AP (i.e., the number of supported streams) that forces the AP to ignore some of the received RTS frames. Therefore, the contention stage should be at least Nm to enable the AP to serve Nm uplink stations, but it should not be extremely high to avoid an increase in packet delay.

2) Full Duplex Vs. Half Duplex Multi-Band Operation: We now compare the proposed IBFD MAC protocol with a half-duplex AP using similar frame structures. The main difference is that the half-duplex operation on the mmWave data transmission stage is divided into one uplink period and another downlink period to serve the half-duplex stations. The IBFD configuration outperforms the half-duplex configuration by an average of 85%, as shown in Fig. 11(b). The gain peaks at 101%, which is just more than twice the half-duplex performance with twenty stations.

3) Effect of Channel Errors: The AP sets the data transmission rate for each station after acquiring the channels of all uplink and downlink stations. However, there may be errors in the acquired channel. These erroneous channel estimates can result in a mismatch between the selected and achievable rates using inaccurate beamforming. In our simulation, we model the channel errors as follows. (i.) Overestimated error: The transmitter sends at a transmission rate higher than the station's supported rate. As a result, the receiver

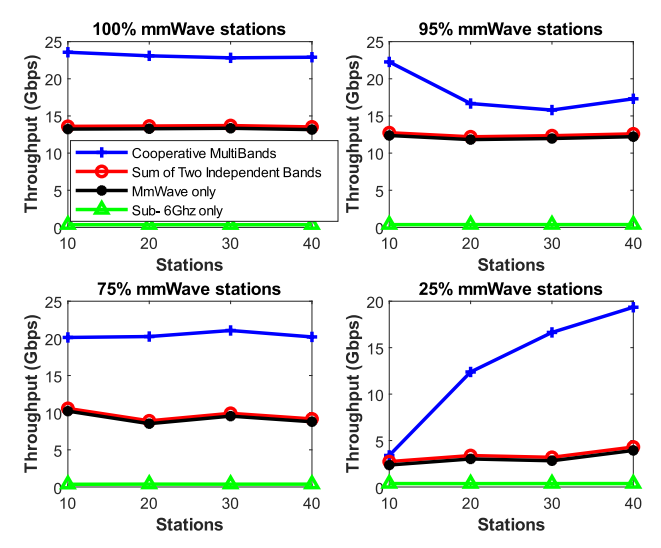


Fig. 12. Throughput result for MB-FDMAC and FD-MUMAC with different number of in mmWave range station.

cannot decode the received data, which results in lost packets. (ii.) Underestimated error: The transmitter sends with a lower transmission rate than the maximum supported rate, lowering the transmission efficiency but not losing packets. In both cases, the erroneous rates are selected randomly from the possible rate choices. Fig. 11(c) shows that MB-FDMAC throughput degrades as the probability of channel errors (Pe) increases. However, the channel error effect is limited to the affected stations' throughputs.

- 4) Effect of RTS Collison During the Contention Stage: In this subsection, we analyze the effect of the RTS transmission collision that occurs when two stations attempt to send an RTS frame simultaneously, which results in lost RTS packets. Fig. 11(d) shows the successful RTS frames transmission of the MB-JSS and the Random schemes close to each other. However, using the MB-JSS scheme reduces the lost packets significantly, as shown by the error bars that are related to the left y-axis. Also, the MB-JSS scheme reduces the stations' average CW size by more than 33%, significantly reducing the waiting time before sending an RTS frame, as shown in the right y-axis in Fig. 11(d).
- 5) Cooperative Versus Individual Dual Bands Operation: To evaluate the effectiveness of the multi-band operation, we compare MB-FDMAC with FDMUMAC, which enables an IBFD AP to serve multiple stations by using the MB-JSS method. We run FDMUMAC in the sub-6 GHz and mmWave bands separately. We use four baselines for placement of the stations in our simulation, where the percentage of stations in the mmWave range are: 100%, 95%, 75%, and 25% serving as a way to compare with the operation in the sub-6 GHz band only. Fig. 12 depicts the performance of MB-FDMAC and FDMUMAC under the aforementioned parameters where Cooperative Multi-Band represents MB-FDMAC, Independent Two Bands represents the sum of FDMUMAC throughput in mmWave, and sub- 6GHz, MmWave only for FDMUMAC in mmWave band, and sub-6GHz represents FDMUMAC in the sub-6GHz band. MB-FDMAC outperforms the combined results of FDMUMAC in the sub-6 GHz and mmWave bands by 87% with stations that are all mmWave complaints. The

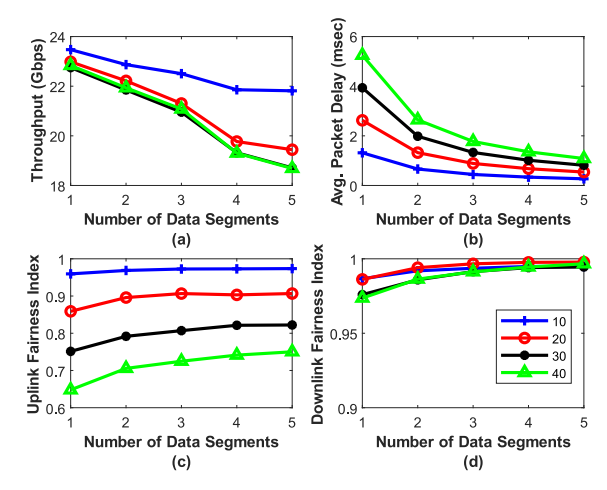


Fig. 13. Simulation results vs. the number of data stage segments: (a) Throughput, (b) Average packet delay, (c) Uplink fairness, (d) Downlink fairness.

MB-FDMAC gain comes from removing the wasted time of transmitting control frames on the mmWave band since the standard requires using the lowest modulation scheme to transmit the control frames. Therefore, the enormous instantaneous mmWave bandwidth is wasted by sending just a few control data bits. Adding sub-6 GHz only stations result in a throughput degradation, as shown in Fig. 12. With 25% of the stations in the mmWave range, the gain of MB-FDMAC reduced to 12% compared with combining the throughput of FDMUMAC in the sub-6 GHz and mmWave bands. This reduction is due to the small number of stations that take advantage of the mmWave band. However, with an increase in the number of stations, the gain increases significantly since more stations capitalize on the high data rates of the mmWave band.

D. MB-FDMAC With Multiple Data Stage Segments

In this subsection, we quantify the effect of dividing the data transmission stage into V segments, which is presented in Section IV-C We evaluate the throughput, average packet delay, and fairness for MB-JSS with a different number of segments.

- 1) Throughput: The throughput slightly declines with an increase in V, as shown in Fig. 13(a), due to the following factors: (i.) the increase of the beamforming overhead with a large number of stations, and (ii) the RIFS waiting time that separates two data segments. However, these two factors do not result in a significant degradation in throughput. For example, increasing V by one reduces the throughput by an average of only 5.5%.
- 2) Delay: As shown in Fig. 13(b), the average packet delay decreases substantially as T_0 increases. For example, with 40 stations, the average packet delay reduces by 49.5% simply by increasing V by one. Furthermore, the delay reduces by 80% with V=5 compared to V=1. The delay reduction comes from the AP's ability to serve more stations during the mmWave data transmission stage, which reduces the number of rejected stations from the uplink transmission.
- 3) Fairness: Fig. 13 (c and d) show that the uplink and downlink fairness has improved by increasing V. For example,

Fig. 13(c) shows an improvement in uplink fairness by 5% in fairness by increasing V by one for 40 stations and reaching a 12.5% improvement for V=5.

E. MB-JSS Complexity Analysis

The main objective of MB-JSS is to find multiple combinations of stations to serve these stations either in the mmWave band or μ Wave band while ensuring fairness. To be precise, in analyzing MB-JSS complexity, we divide the algorithm to uplink and downlink stations selection on each band. For the uplink station selection, MB-JSS sorts the stations based on their uplink deficit. Then, MB-JSS selects only the stations with the highest deficit to be served for the uplink transmission. Hence, the complexity of MB-JSS is $O(N^2)$. However, the growth of N is upper bounded by the number of received RTS frames from the uplink stations, which reduces the complexity of MB-JSS significantly. On the other hand, the AP feeds MB-JSS a predetermined list of stations that have the highest downlink deficit, which eliminates using the computational resource to find the downlink station. Finally, the procedure of ensuring that every selected uplink station is not designated as a downlink station - since the stations are half duplex stations- has a worst-case scenario complexity of O(N) where N is limited by the number of uplink contention winners. Based on this analysis, applying MB-JSS is feasible to implement without any complexity concerns.

VII. CONCLUSION

In this paper, we proposed a fully integrated MAC protocol, MB-FDMAC, for an IBFD AP that serves multiple uplink and downlink stations by mainly using the sub-6 GHz band to transmit control frames and the mmWave band to transmit data frames. We presented the benefits of using MB-FDMAC for dual-band networks and quantified its advantages over a protocol that works separately in the two bands. Also, we proposed a joint station selection algorithm that ensures fairness among all stations in the network and balances each station's uplink and downlink traffic. Then, we provided extensive simulations for MB-FDMAC under different conditions. In addition, we showed the benefits of the proposed selection scheme in reducing the effect of RTS frame collision. Finally, we showed a time segmenting feature for MB-FDMAC that reduced packet delay and increased fairness while maintaining the throughput. In future work, we plan to study a variation of MB-FDMAC in an environment that uses cooperative access points.

REFERENCES

- [1] Cisco. (2020). Cisco: 2020 CISO Benchmark Report. [Online]. Available: http://dx.doi.org/10.1016/s1361-3723(20)30026-9
- [2] Statista. (2021). Data Volume of Global Internet Video to TV Traffic From 2016 to 2021. [Online]. Available: https://www.statista. com/statistics/267222/global-data-volume-of-internet-video-to-tv-traffic/
- [3] D. Wang and C. H. Chan, "Multiband antenna for WiFi and WiGig communications," *IEEE Antennas Wireless Propag. Lett.*, vol. 15, pp. 309–312, 2016, doi: 10.1109/LAWP.2015.2443013.
- [4] A. Ali, N. González-Prelcic, and R. W. Heath, "Estimating millimeter wave channels using out-of-band measurements," in *Proc. Inf. Theory Appl. Workshop (ITA)*, Jan. 2016, pp. 1–6, doi: 10.1109/ITA.2016.7888146.

- [5] O. Semiari, W. Saad, and M. Bennis, "Joint millimeter wave and microwave resources allocation in cellular networks with dual-mode base stations," *IEEE Trans. Wireless Commun.*, vol. 16, no. 7, pp. 4802–4816, Jul. 2017, doi: 10.1109/TWC.2017.2703109.
- [6] G. H. Sim, T. Nitsche, and J. C. Widmer, "Addressing MAC layer inefficiency and deafness of IEEE802.11ad millimeter wave networks using a multi-band approach," in *Proc. IEEE 27th Annu. Int. Symp. Pers., Indoor, Mobile Radio Commun. (PIMRC)*, Sep. 2016, pp. 1–6, doi: 10.1109/PIMRC.2016.7794830.
- [7] S. Buzzi, C. D'Andrea, M. Fresia, and X. Wu, "Multi-UE multi-AP beam alignment in user-centric cell-free massive MIMO systems operating at mmWave," *IEEE Trans. Wireless Commun.*, vol. 21, no. 11, pp. 8919–8934, Nov. 2022, doi: 10.1109/TWC.2022.3170787.
- [8] O. Semiari, W. Saad, M. Bennis, and M. Debbah, "Integrated millimeter wave and sub-6 GHz wireless networks: A roadmap for joint mobile broadband and ultra-reliable low-latency communications," *IEEE Wireless Commun.*, vol. 26, no. 2, pp. 109–115, Apr. 2019, doi: 10.1109/MWC.2019.1800039.
- [9] S. Aggarwal, S. K. Saha, I. Khan, R. Pathak, D. Koutsonikolas, and J. Widmer, "MuSher: An agile multipath-TCP scheduler for dual-band 802.11ad/AC wireless LANs," *IEEE/ACM Trans. Netw.*, vol. 30, no. 4, pp. 1879–1894, Aug. 2022, doi: 10.1109/TNET.2022. 3158678.
- [10] O. Semiari, W. Saad, M. Bennis, and M. Debbah, "Performance analysis of integrated sub-6 GHz-millimeter wave wireless local area networks," in *Proc. IEEE Global Commun. Conf.*, Dec. 2017, pp. 1–7, doi: 10.1109/GLOCOM.2017.8254610.
- [11] Á. López-Raventós and B. Bellalta, "Dynamic traffic allocation in IEEE 802.11be multi-link WLANs," *IEEE Wireless Commun. Lett.*, vol. 11, no. 7, pp. 1404–1408, Jul. 2022, doi: 10.1109/LWC.2022. 3171442.
- [12] P. Zhou, X. Fang, and X. Wang, "Joint radio resource allocation for decoupled control and data planes in densely deployed coordinated WLANs," *IEEE Trans. Wireless Commun.*, vol. 20, no. 6, pp. 3749–3759, Jun. 2021, doi: 10.1109/TWC.2021.3053354.
- [13] P. Zhou et al., "IEEE 802.11ay-based mmWave WLANs: Design challenges and solutions," *IEEE Commun. Surveys Tuts.*, vol. 20, no. 3, pp. 1654–1681, 3rd Quart., 2018.
- [14] H. Zhai, J. Wang, and Y. Fang, "DUCHA: A new dual-channel MAC protocol for multihop ad hoc networks," *IEEE Trans. Wireless Commun.*, vol. 5, no. 10, pp. 3224–3233, Nov. 2006, doi: 10.1109/TWC.2006.04869.
- [15] D. Gesbert, M. Kountouris, R. W. Heath, C.-B. Chae, and T. Salzer, "Shifting the MIMO paradigm," *IEEE Signal Process. Mag.*, vol. 24, no. 5, pp. 36–46, Sep. 2007, doi: 10.1109/MSP.2007.904815.
- [16] R. Liao, B. Bellalta, M. Oliver, and Z. Niu, "MU-MIMO MAC protocols for wireless local area networks: A survey," *IEEE Commun. Surveys Tuts.*, vol. 18, no. 1, pp. 162–183, 1st Quart., 2016, doi: 10.1109/COMST.2014.2377373.
- [17] A. Sabharwal, P. Schniter, D. Guo, D. W. Bliss, S. Rangarajan, and R. Wichman, "In-band full-duplex wireless: Challenges and opportunities," *IEEE J. Sel. Areas Commun.*, vol. 32, no. 9, pp. 1637–1652, Sep. 2014, doi: 10.1109/JSAC.2014.2330193.
- [18] F. U. Din and F. Labeau, "Artificial noise assisted in-band full-duplex secure channel estimation," *IEEE Trans. Veh. Technol.*, vol. 70, no. 7, pp. 6800–6813, Jul. 2021, doi: 10.1109/TVT.2021.3082810.
- [19] D. Kim, H. Lee, and D. Hong, "A survey of in-band full-duplex transmission: From the perspective of PHY and MAC layers," *IEEE Commun. Surveys Tuts.*, vol. 17, no. 4, pp. 2017–2046, 4th Quart., 2015, doi: 10.1109/COMST.2015.2403614.
- [20] K. E. Kolodziej, B. T. Perry, and J. S. Herd, "In-band full-duplex technology: Techniques and systems survey," *IEEE Trans. Microw. Theory Techn.*, vol. 67, no. 7, pp. 3025–3041, Jul. 2019, doi: 10.1109/TMTT.2019.2896561.
- [21] A. Tang and X. Wang, "A-duplex: Medium access control for efficient coexistence between full-duplex and half-duplex communications," *IEEE Trans. Wireless Commun.*, vol. 14, no. 10, pp. 5871–5885, Oct. 2015, doi: 10.1109/TWC.2015.2443792.
- [22] M. Peng et al., "A spatial group-based multi-user full-duplex OFDMA MAC protocol for the next-generation WLAN," Sensors, vol. 20, no. 14, p. 3826, 2020, doi: 10.3390/s20143826.
- [23] Q. Qu, B. Li, M. Yang, Z. Yan, and X. Zuo, "MU-FuPlex: A multiuser full-duplex MAC protocol for the next generation wireless networks," in *Proc. IEEE Wireless Commun. Netw. Conf. (WCNC)*, Mar. 2017, pp. 1–6, doi: 10.1109/WCNC.2017.7925936.

- [24] M. Peng et al., "A trigger-free multi-user full duplex user-pairing optimizing MAC protocol," in *Proc. Int. Conf. Internet Things Service*. Cham, Switzerland: Springer, 2019, pp. 598–610, doi: 10.1007/978-3-030-44751-9 51.
- [25] W. Kim, T. Kim, S. Joo, and S. Pack, "An opportunistic MAC protocol for full duplex wireless LANs," in *Proc. Int. Conf. Inf. Netw. (ICOIN)*, Jan. 2018, pp. 810–812, doi: 10.1109/ICOIN.2018.8343230.
- [26] Y. Alkhrijah, J. Camp, and D. Rajan, "Full duplex multiuser MIMO MAC protocol (FD-MUMAC)," in *Proc. IEEE Global Commun. Conf.*, Dec. 2020, pp. 1–6, doi: 10.1109/GLOBECOM42002.2020.9348214.
- [27] C. Deng et al., "IEEE 802.11be Wi-Fi 7: New challenges and opportunities," *IEEE Commun. Surveys Tuts.*, vol. 22, no. 4, pp. 2136–2166, 4th Quart., 2020, doi: 10.1109/COMST.2020.3012715.
- [28] E. Khorov, I. Levitsky, and I. F. Akyildiz, "Current status and directions of IEEE 802.11be, the future Wi-Fi 7," IEEE Access, vol. 8, pp. 88664–88688, 2020, doi: 10.1109/access.2020.2993448.
- [29] M. Un, W. Ma, and P. C. Ching, "Joint transmit beamforming optimization and uplink/downlink user selection in a full-duplex multi-user MIMO system," in *Proc. IEEE Int. Conf. Acoust.*, *Speech Signal Process. (ICASSP)*, Mar. 2017, pp. 3639–3643, doi: 10.1109/ICASSP.2017.7952835.
- [30] J. Kim, W. Choi, and H. Park, "Beamforming for full-duplex multiuser MIMO systems," *IEEE Trans. Veh. Technol.*, vol. 66, no. 3, pp. 2423–2432, Mar. 2017, doi: 10.1109/TVT.2016.2581213.
- [31] IEEE Standard for Information Technology-Telecommunications and Information Exchange between Systems Local and Metropolitan Area Networks-Specific Requirements Part 11: Wireless LAN Medium Access Control (MAC) and Physical Layer (PHY) Specifications Amendment 1: Enhancements for High-Efficiency WLAN, IEEE Standard 802.11ax-2021, May 2021, pp. 1–767, doi: 10.1109/IEEESTD.2021.9442429.
- [32] K. Satyanarayana, M. El-Hajjar, P. Kuo, A. Mourad, and L. Hanzo, "Hybrid beamforming design for full-duplex millimeter wave communication," *IEEE Trans. Veh. Technol.*, vol. 68, no. 2, pp. 1394–1404, Feb. 2019, doi: 10.1109/TVT.2018.2884049.
- [33] I. P. Roberts and S. Vishwanath, "Beamforming cancellation design for millimeter-wave full-duplex," in *Proc. IEEE Global Commun. Conf. (GLOBECOM)*, Dec. 2019, pp. 1–6, doi: 10.1109/GLOBE-COM38437.2019.9013116.
- [34] M. K. Samimi and T. S. Rappaport, "3-D millimeter-wave statistical channel model for 5G wireless system design," *IEEE Trans. Microw. Theory Techn.*, vol. 64, no. 7, pp. 2207–2225, Jul. 2016, doi: 10.1109/TMTT.2016.2574851.
- [35] J.-S. Jiang and M. A. Ingram, "Spherical-wave model for short-range MIMO," *IEEE Trans. Commun.*, vol. 53, no. 9, pp. 1534–1541, Sep. 2005, doi: 10.1109/TCOMM.2005.852842.
- [36] IEEE Standard for Information Technology—Telecommunications and Information Exchange between Systems Local and Metropolitan Area Networks—Specific Requirements Part 11: Wireless LAN Medium Access Control (MAC) and Physical Layer (PHY) Specifications Amendment 2: Enhanced Throughput for Operation in License-exempt Bands above 45 GHz, IEEE Standard 802.11ay-2021, Jul. 2021, pp. 1–768, doi: 10.1109/IEEESTD.2021.9502046.
- [37] W. Ouyang, J. Bai, and A. Sabharwal, "Leveraging one-hop information in massive MIMO full-duplex wireless systems," *IEEE/ACM Trans. Netw.*, vol. 25, no. 3, pp. 1528–1539, Jun. 2017, doi: 10.1109/TNET.2017.2648878.
- [38] M. Shreedhar and G. Varghese, "Efficient fair queuing using deficit round-robin," *IEEE/ACM Trans. Netw.*, vol. 4, no. 3, pp. 375–385, Jun. 1996, doi: 10.1109/90.502236.
- [39] K. Aldubaikhy et al., "MAC layer design for concurrent transmissions in millimeter wave WLANs," in *Proc. IEEE/CIC Int. Conf. Commun. China* (ICCC), Oct. 2017, pp. 1–6, doi: 10.1109/ICCChina.2017.8330449.
- [40] Y. Zhao, X. Xu, Y. Su, L. Huang, X. Du, and N. Guizani, "Multiuser MAC protocol for WLANs in MmWave massive MIMO systems with mobile edge computing," *IEEE Access*, vol. 7, pp. 181242–181256, 2019, doi: 10.1109/ACCESS.2019.2952174.

[41] R. Jain et al., "A quantitative measure of fairness and discrimination for resource allocation in shared computer systems," 1984, arxiv:cs/9809099.



Yazeed Alkhrijah (Member, IEEE) received the B.S. degree in electrical engineering (communication and electronics) from King Saud University, Riyadh, Saudi Arabia, the M.S. degree in electrical and computer engineering from The University of Tennessee Knoxville, TN, USA, and the Ph.D. degree in electrical and computer engineering with Southern Methodist University, Dallas, TX, USA. In 2022, he was an Assistant Professor with Imam Muhammad Ibn Saud Islamic University, Riyadh. His current research interests include wireless com-

munication, digital signal processing, and digital image processing.



Joseph Camp (Member, IEEE) received the B.S. degree (Hons.) in electrical and computer engineering from UT-Austin, Austin, TX, USA, and the M.S. and Ph.D. degrees in electrical and computer engineering from Rice University, Houston, TX, USA. He is currently the Ad Interim Department Chair of electrical and computer engineering with Southern Methodist University, Dallas, TX, USA. In 2009, he joined the SMU Faculty. His research team has performed more than 200 million in-field wireless measurements around the world via android

deployment and local characterization via drones, campus buses, vehicles, and buildings. His current research interests include wireless communications and networking, crowdsourcing, and drones, specifically focused on the deployment, measurement, and analysis of large-scale systems and the development of embedded protocols. He received the Ralph Budd Award for the Best Engineering Thesis at Rice University in 2010, the National Science Foundation CAREER Award in 2012, the Golden Mustang Teaching Award in 2014, and the Gerald J. Ford Research Fellowship in 2021.



Dinesh Rajan (Senior Member, IEEE) received the B.Tech. degree in electrical engineering from the Indian Institute of Technology Madras, Chennai, India, and the M.S. and Ph.D. degrees in electrical and computer engineering from Rice University, Houston, TX, USA. He is currently the Senior Associate Dean with the Lyle School of Engineering, Southern Methodist University, Dallas, TX, USA. He is also a Cecil and Ida Green Professor with the Electrical and Computer Engineering Department, Southern Methodist University. In August 2002,

he joined the Electrical Engineering Department, Southern Methodist University, as an Assistant Professor. His current research interests include communications theory, wireless networks, information theory, and computational imaging. He was a recipient of the NSF CAREER Award for his work on applying information theory to the design of mobile wireless networks. He was also a recipient of the Golden Mustang Outstanding Faculty Award and the Senior Ford Research Fellowship from SMU.